



# 2D/3D Shaped Radiation Patterns of Sunflower and Conformal Antenna Arrays Using Phase Synthesis

Saber Helmy Zainud-Deen<sup>1,2</sup> · Doaa Mohammed Zaki Azzam<sup>2</sup> ·  
Hend Abd El-Azem Malhat<sup>2</sup> 

© Springer Science+Business Media, LLC, part of Springer Nature 2020

## Abstract

2D and 3D beam synthesis from different antenna array arrangements are investigated in this paper. Planar sunflower, conformal cylindrical and spherical helical array arrangements are studied. The particle swarm optimization (PSO) technique is used to predict the phase distribution on the array elements. The beam synthesis is achieved by comparing the array factor with a predetermined mask with both upper and lower limits according to the intended application requirements. Different 2D and 3D masks are used in beam synthesis as pencil, flat-top, and cosecant single beam are predicted. The planar sunflower antenna array is investigated due to its high gain, low side-lobe level (SLL) below  $-20$  dB and its compact size. The phase distribution of sunflower array is estimated using PSO to radiate dual-beams in different planes. Dual-beam with pencil, flat-top, and cosecant beams are obtained with different half-power beam widths. 3D conformal antenna arrays of cylindrical and spherical helical arrangements are studied. Each 3D conformal array consists of four arms shifted in position by  $90^\circ$  orientation angle. Each arm is designed to radiate single beam in a specific direction. Four-beams are considered to radiate in the directions of  $\theta_{1,2,3,4}=30^\circ$ , and  $\phi_1=0^\circ$ ,  $\phi_2=90^\circ$ ,  $\phi_3=180^\circ$ , and  $\phi_4=270^\circ$  with SLL optimized below  $-17$  dB. The array arrangements analysis is based on the array theory formulation, through the implementation of the estimated equation using a home programmed MATLAB code.

**Keywords** Particle swarm optimization · 3D conformal array · Sunflower array · Beam synthesis

## 1 Introduction

Recently, the problem of pattern synthesis of antenna arrays attracts the researcher's attention in different communications area [1]. Pattern synthesis is employed in modern wireless communication systems such as radar, satellite communications, millimeter wave

---

✉ Hend Abd El-Azem Malhat  
er\_honidal@yahoo.com

Saber Helmy Zainud-Deen  
anssaber@yahoo.com

<sup>1</sup> Faculty of Engineering and Technology, Badr University in Cairo (BUC), Badr, Egypt

<sup>2</sup> Faculty of Electronic Engineering, Menoufia University, Menouf, Egypt

communications and weather radar. Reconfigurable antennas with shaped patterns are the suitable solution for moving target applications, where the antenna beam is continuously steered towards the transmitter or receiver. Pattern synthesis determine the beam shape, half-power beam-width (HPBW), direction, and side-lobe level (SLL), back-lobe level according to the requirements of each application [2]. The beam synthesis techniques are focused on estimating the relationship between the far-field pattern of an antenna array and the corresponding amplitude and phase distributions of the individual elements. Those techniques which deals with the phase distribution only with equal magnitudes of the array elements, are called phased antenna arrays (PA) [3]. The pattern synthesis techniques are achieved by the proper design of the phase shift between the array elements in the feeding network. PA introduces radiations with controlled beam size and beam shape according to the number of elements and their spacing [4]. When the number of the array elements is increased, the gain is increased, and the SLL is decreased. The main disadvantage of PA's is the large number of phase shifters and control units employed in the structure which increase the total fabrication cost.

The antenna arrays are classified according to the spacing between elements into uniform and non-uniform arrays. Most of beam synthesis techniques are applied to uniform antenna arrays due to their simple analysis [5]. Different optimization algorithms are used to estimate the array elements phase distribution as illustrated in [6]. Uniform arrays suffer from power loss in grating lobes for element spacing larger than half wavelength [7]. Aperiodic arrangements of the array elements are used to reduce its size, reduce the SLL and eliminate the grating lobes [8]. Antenna arrays have different arrangements in 1D (linear), 2D (planar), and 3D according to elements placement [9]. Conformal antennas are being used for the wireless applications that require an antenna to operate on a surface which is not flat. Conformal arrays are employed in some applications as missiles, biomedical systems, aircraft, remote sensing, and satellites communications [10]. The pattern of multiplication and array factor theory are used in 2D and 3D array analysis [11]. Conformal array analysis can't be expressed by a simple polynomial due to the illumination around the curved radiating surface, and the polarization of each element [12].

This paper introduces an expansion of the study introduced in [13] with deep explanation of the obtained results. This paper formulate a mathematical analysis of the beam syntheses array in 2D and 3D arrangements in details. Pattern synthesis for 2D sunflower and 3D conformal array arrangements using phase control is investigated. Beam synthesis in 2D array arrangement in 2 planes with dual beams of different beamwidths are investigated. The beam shaping with nulls for noise reduction is investigated and the results are introduced. Analysis of 3D array arrangement include curved structure with 3D beam shaping of different beamwidths. 3D cylindrical and spherical helical array arrangements, with shaped radiation patterns are studied. The PSO algorithm is employed to predict the phase distribution on antenna arrays. The analysis of different arrays was implemented using home programmed MATLAB code deals with the array factors only.

## 2 Problem Formulation and Optimization Technique

The array factor (AF) is used to calculate the total field radiated from the antenna array. The total field is achieved by multiplying the field of a single element by the AF. Assume that, an antenna array consists of  $N$  isotropic elements excited by the same amplitudes, and different phases. The isotropic single element which has a radiated field as,  $\frac{e^{-jkr}}{4\pi r}$ , produce

constant radiation intensity (isotropic). The array elements are excited with a signal at an amplitude of 1, and different phase shift due to the un-equal transmission paths between. The AF can be written as

$$\begin{aligned} AF &= e^{jkr_1^\wedge \cdot a^\wedge} + e^{jkr_2^\wedge \cdot a^\wedge} + e^{jkr_3^\wedge \cdot a^\wedge} + \dots e^{jkr_{N-1}^\wedge \cdot a^\wedge} \\ &= \sum_{i=1}^N e^{jkr_i^\wedge \cdot a^\wedge} \end{aligned} \quad (1)$$

where  $r_i$  is the position vector of antenna elements,  $k = \frac{2\pi}{\lambda}$  is the wave number,  $a^\wedge$  is the unit vector pointing the  $i$ th element positioned at  $(x_i, y_i, z_i)$  to the array axis

$$r_i^\wedge = x_i a_x^\wedge + y_i a_y^\wedge + z_i a_z^\wedge \quad (2)$$

$$a^\wedge = \sin(\theta) \cos(\vartheta) a_x^\wedge + \sin(\theta) \sin(\vartheta) a_y^\wedge + \cos(\theta) a_z^\wedge \quad (3)$$

The general AF of antenna array is calculated by:

$$AF = \sum_{i=1}^N e^{j k x_i u} e^{j k y_i v} e^{j k z_i \sqrt{1-u^2-v^2}} e^{j \alpha_i} \quad (4)$$

where  $u = \cos\theta \sin\vartheta$ ,  $v = \sin\theta \sin\vartheta$ , and  $w = \cos\theta$ ,  $\vartheta = \tan^{-1}\left(\frac{v}{u}\right)$ , and  $\theta = \cos^{-1} \sqrt{1 - (u^2 + v^2)}$ . The maximum extend of the pattern-space is defined by  $u^2 + v^2 + w^2 = 1$ . Thus the total field can be found from:

$$E_t = \text{field of single element} \times AF \quad (5)$$

The PSO technique is used for estimation of the elements phases to obtain the shaped beams in different directions to solve the complex problems of array adaptation.

## 2.1 Particle Swarm Optimization (PSO) Technique

PSO is a simple parallel processing optimization algorithm, with detailed analysis introduced in [14]. In PSO, the problem starts with population of random particles and searches for optimum values through updating the generations. Each particle remembers its best solution called personal best ( $P$ ) and the global best ( $P_g$ ) which is the best solution achieved so far by any of the individuals. At each iteration, the particles update their velocities towards the global location according to the following two equations [15]:

$$v_i^{n+1} = \left[ \omega v_i^n + \frac{c_1 r_1^n (P_i^n - x_i^n) + c_2 r_2^n (P_g^n - x_i^n)}{\Delta t} \right] \quad (6)$$

$$x_i^{n+1} = x_i^n + v_i^{n+1} \cdot \Delta t \quad (7)$$

where  $v_i^n$  and  $x_i^n$  are the particle velocity and position at the  $n$ th generation, respectively.  $\omega$  is the inertia weight of particles in the range of  $[0, 1]$ .  $c_1=c_2=2.0$  are scaling constants,  $r_1=r_2=4$  are random numbers uniformly distributed in  $(0,1)$ .  $P_k^n$  best “remembered individual particle position,  $P_k^n$  best remembered swarm position. The radiated beam from a specific array arrangement is defined by a mask with upper limit,  $M_U$ , and lower limit,  $M_L$ , according to the constrains:

$$M_L(u, v) \leq |AF(u, v)| \leq M_U(u, v) \quad (8)$$

The PSO optimization is performed to minimize the square root of the norm  $F$

$$F = \sum_{n=1}^{N_f} \left[ (AF(u, v) - M_U(u, v))^2 + (AF(u, v) - M_L(u, v))^2 \right] \quad (9)$$

where  $N_f$  is the number of points,  $AF(u, v)$  is the estimated array factor using PSO. In this paper, 2D and 3D masks are produced from different array configuration in 2-D and 3-D surfaces.

### 3 Planar Sunflower Array

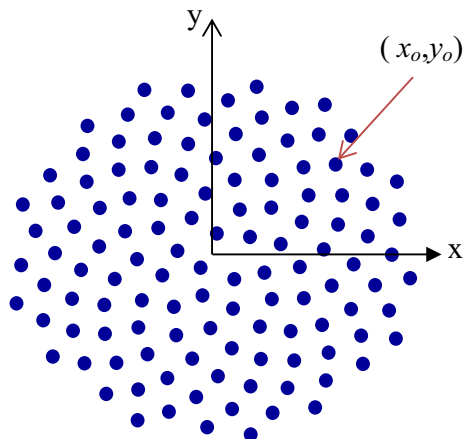
#### 3.1 2-D Radiation Pattern Synthesis

The non-uniform arrays (NUA) have the ability to offer a comparable performance to that of a uniform arrays, but with a reduced number of physical elements. The sunflower array has non-uniform arrangement according to the polar equations  $(r, \theta)$  of the  $i$ th elements given by [16, 17],

$$r = \frac{s}{\sqrt{\pi}} \sqrt{m} \quad m = 1, 2, \dots, N$$

$$\theta = 2\pi m\tau \quad (10)$$

**Fig. 1** The 2D sunflower array elements arrangement



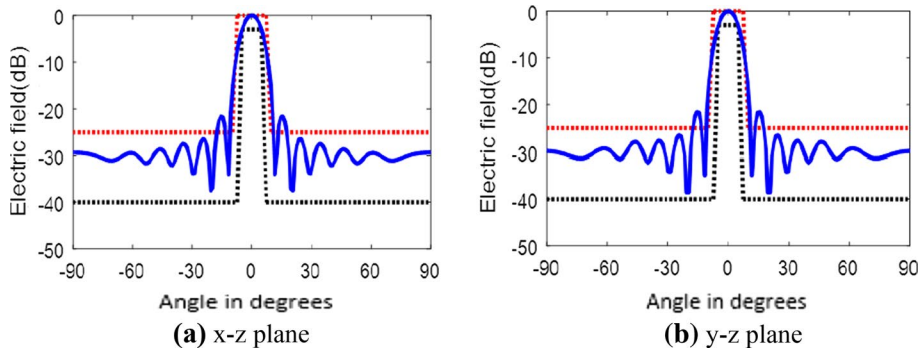


**Fig. 2** The synthesized pattern for 2D sunflower array with pencil beam of HPBW 20°

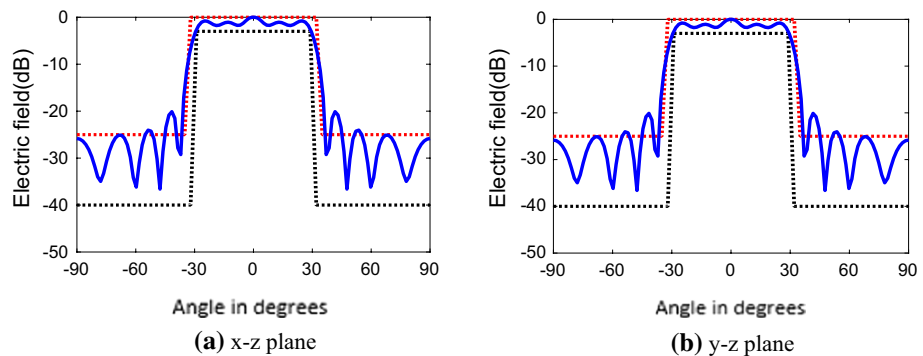


**Fig. 3** The synthesized pattern for 2D sunflower array with flat-top beam of HPBW 60°

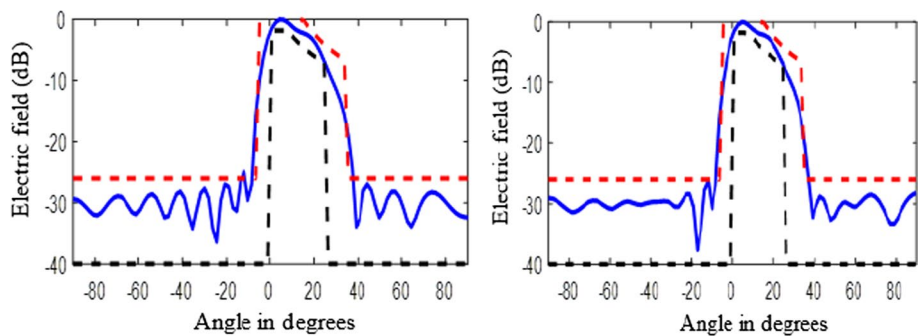


**Fig. 4** The synthesized pattern for 2D sunflower array with single cosecant squared shaped beam

where  $s$  is the linear spacing between elements,  $m$  is the number of elements in the array, and  $\tau$  is the golden ratio of 1.618. The sunflower arrangement with  $N=121$  element, and  $s=0.27\lambda$  at 12 GHz is plotted in Fig. 1.

Figure 2 shows the synthesized electric field using PSO and the designed mask of a single pencil beam in x-z plane and y-z planes. A 2D mask with half-power beam width

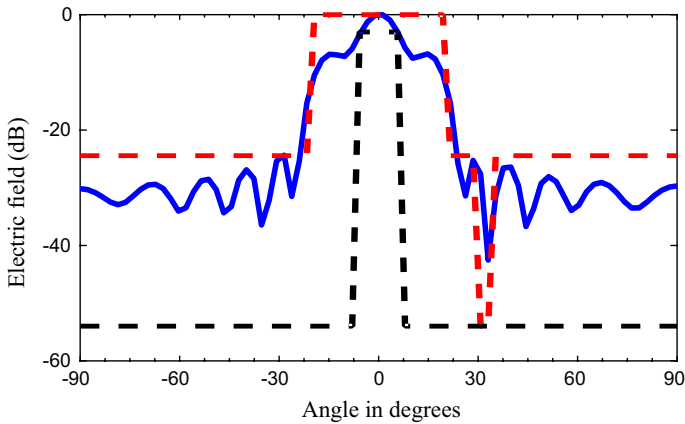


**Fig. 5** The electric field pattern versus elevation angle for 2D sunflower array with narrow null at  $30^\circ$

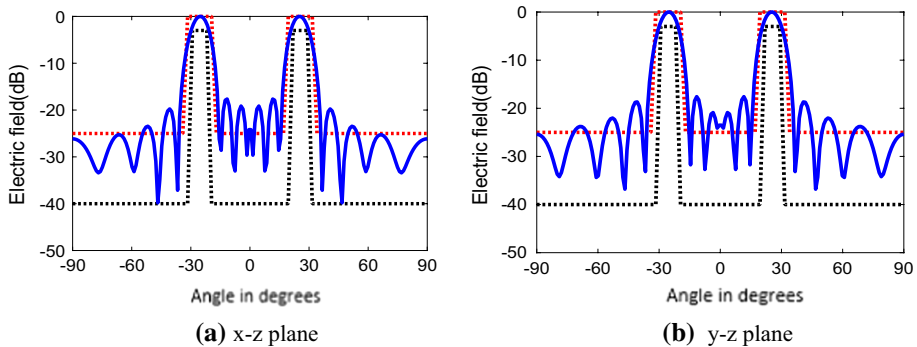


**Fig. 6** The synthesized patterns for 2D sunflower array with dual beams at  $\pm 25^\circ$  and  $\text{HPBW} = 20^\circ$

(HPBW) of  $20^\circ$  and  $-40 \text{ dB} \leq \text{SLL} \leq -25 \text{ dB}$  is employed in the two planes. The estimated electric field patterns satisfy the mask requirements with first SLL of  $-22 \text{ dB}$  and HPBW of  $20^\circ$ . Figure 3 introduces 2D single flat-top beam mask with constraints of HPBW of  $60^\circ$  and  $-40 \text{ dB} \leq \text{SLL} \leq -25 \text{ dB}$  using dashed lines and the estimated beam using PSO appeared as a solid line. The synthesized pattern falls between the bounds of the shaped region with small ripples. For radar applications, cosecant squared pattern is required which is shown in Fig. 4, where the mask limits track the cosecant square equation, and the radiation pattern flows it to achieve the target.

Many systems are expected to suffer from interference at certain angle, so this interference should be prevented or nulled. Null-steering is a method which enable to do that. PSO select the excitation of each element such that the directional pattern has nulls in particular directions. In this manner, undesirable interference or noise can be reduced or completely eliminated. Figure 5 shows a shaped single beam with narrow null at  $30^\circ$  and SLL below  $-25 \text{ dB}$ .

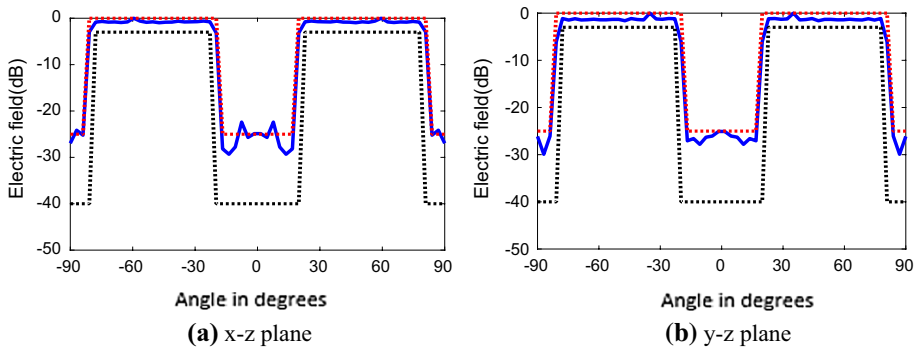


**Fig. 7** The synthesized patterns for 2D sunflower array with dual beams at  $\pm 50^\circ$  and HPBW =  $60^\circ$

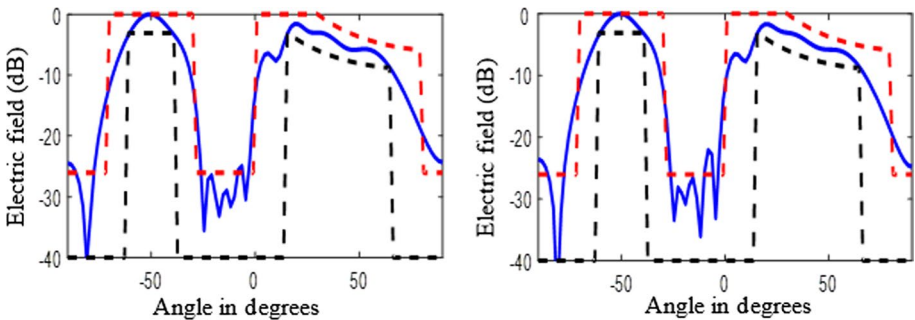


**Fig. 8** The synthesized electric field pattern for 2D sunflower array with two different shaped beams

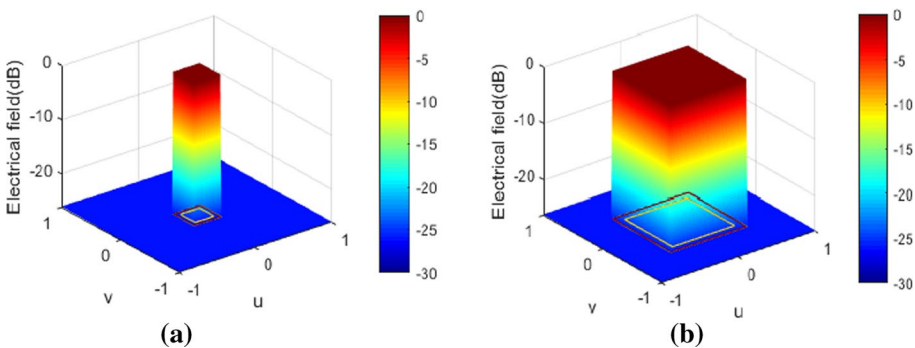


**Fig. 9** The 3D mask pattern for **a** pencil beam, and **b** flat-top beams

The sunflower array elements are excited with equal amplitude signals and different phases to generate dual-beams in in x-z and y-z planes. Figure 6 introduces a synthesized electric field which follows the desired mask in different planes. 2D mask with dual beams at  $\theta = -25^\circ$  and  $\theta = +25^\circ$  and HPBW of  $20^\circ$  and  $-40 \text{ dB} \leq \text{SLL} \leq -25 \text{ dB}$

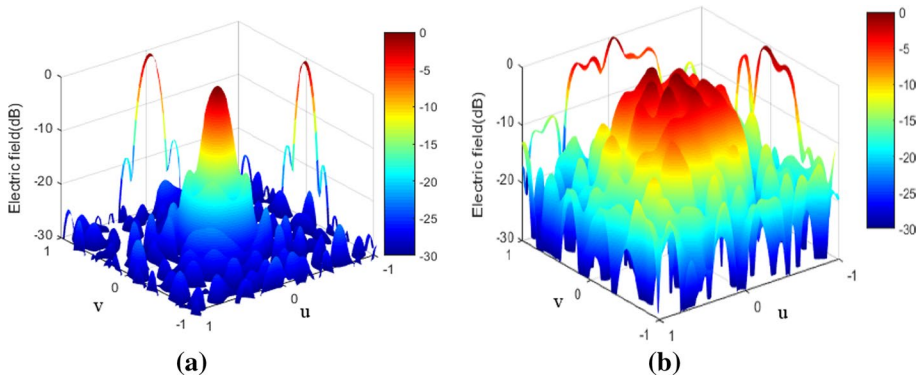


**Fig. 10** The 3D synthesized patterns, **a** pencil beam, and **b** flat-top beam

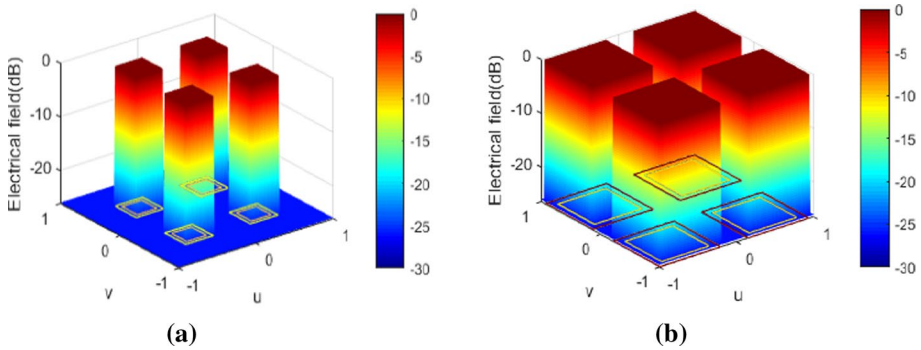


**Fig. 11** The 3D mask pattern for different four beams **a** pencil beam, and **b** flat-top beams

is employed in both  $x$ - $z$  and  $y$ - $z$  planes. The same set of PSO estimated excitations is used for the dual- pencil beams. Similarly, in Fig. 7 dual flat-top beams at  $\theta = -50^\circ$  and  $\theta = +50^\circ$  and HPBW of  $60^\circ$  and  $-40 \text{ dB} \leq \text{SLL} \leq -25 \text{ dB}$  are introduced. The estimated dual-beams are laying within the mask limits in the two planes. In Fig. 8, two different shaped beams in  $x$ - $z$  and  $y$ - $z$  planes are achieved using the 2D sunflower array. A wide beam of HPBW of  $40^\circ$  at  $\theta = -50^\circ$ , and cosecant square beam of HPBW of  $60^\circ$  at  $\theta = +40^\circ$ . The estimated beams exist between the upper and lower boundaries of the masks with  $-40 \text{ dB} \leq \text{SLL} \leq -25 \text{ dB}$ .

### 3.2 3-D Radiation Pattern Synthesis

The 3D beam synthesis of 2D sunflower arrays by adjusting phase distribution according to a designed 3D masks is investigated. The required 3D masks are pencil and a flat-top beams are shown in Fig. 9. The 3D pencil beam has HPBW of  $10^\circ$  and  $-30 \text{ dB} \leq \text{SLL} \leq -20 \text{ dB}$  and the 3D flat-top beam has HPBW of  $60^\circ$  and  $-30 \text{ dB} \leq \text{SLL} \leq -20 \text{ dB}$ . The estimated phase distribution on array elements produces pencil and flat-top 3D beams to satisfy the predetermined masks requirements and plotted in Fig. 10. The SLL is below  $-20 \text{ dB}$  for the pencil beam and below  $-12 \text{ dB}$  for the flat-top beam. 3D mask designed with four



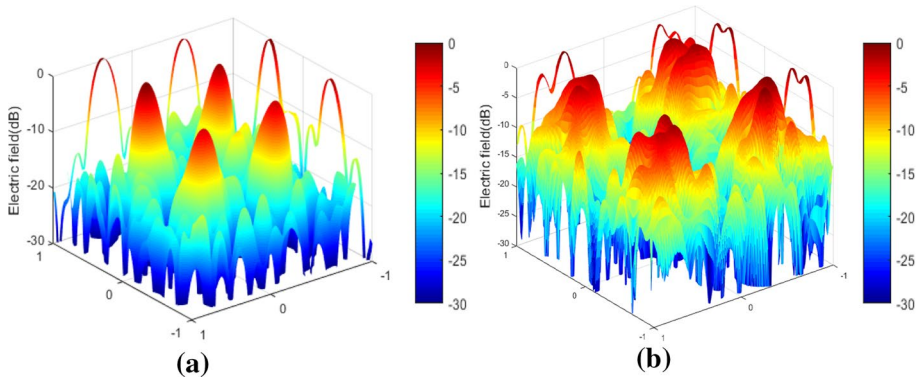


**Fig. 12** The 3D synthesized patterns for different four beams **a** pencil beam, and **b** flat-top beams

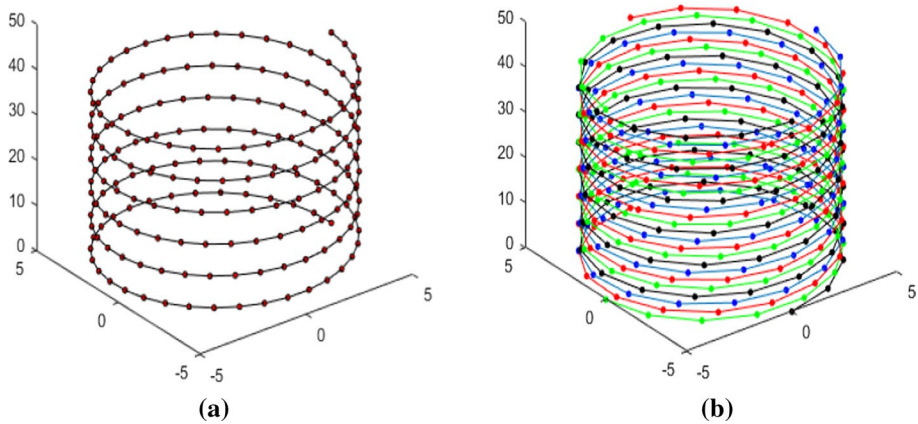


**Fig. 13** The 3D cylindrical helical antenna array **a** single arm, **b** four-orthogonal arms

different beams at  $\theta_{1,2,3,4} = 30^\circ$ , and  $\phi_1 = 0^\circ$ ,  $\phi_2 = 90^\circ$ ,  $\phi_3 = 180^\circ$ , and  $\phi_4 = 270^\circ$  in the same time with is designed for pencil beam of HPBW of  $10^\circ$  and flat-top beam of HPBW of  $40^\circ$  shown in Fig. 11. The generated of four beams patterns radiated by the 2D sunflower array with a common amplitude are illustrated in Fig. 12. Good patterns are achieved with the similar beam characteristics at the four directions.

## 4 3D Pattern Synthesis of Helical Conformal Antenna Arrays

### 4.1 3D Cylindrical Helical Array

3D helical conformal antenna array elements are arranged in a cylindrical structure. Figure 13 shows four identical helical arms positioned with  $90^\circ$  rotation angle to each. The locus of array elements at each helical arm with radius  $R_o$ , and turns  $M$  is given by [18, 19],

$$\begin{aligned}
 x &= R_o \cos(\phi + \pi p/2) \\
 y &= R_o \sin(\phi + \pi p/2) \\
 z &= R_o \phi \tan \alpha
 \end{aligned} \tag{11}$$

where angle  $\phi$  started 0 and ended at  $\phi 2\pi M$ . The helical arm number  $p$  is varied from 0 to 3. The helix has circumference  $C=2\pi R_o$ , pitch angle  $\alpha$ , and spacing between turns  $S=C \tan \alpha$ . The dimensions of the antenna structure are as follows:  $D=5\lambda$ ,  $S=5\lambda$  and  $M=6$  turns, and the number of elements in each arm is  $N=500$ .

Each arm of the 3D cylindrical helical array is designed to radiate a single beam in different directions. Figure 14 shows the estimated pattern of a single beam designed in the directions of  $\theta_{1,2,3,4}=30^\circ$ , and  $\phi_1=0^\circ$  for the first arm ( $p=0$ ),  $\phi_2=90^\circ$  for the second arm ( $p=1$ ),  $\phi_3=180^\circ$  for the third arm ( $p=2$ ) and  $\phi_4=270^\circ$  for the forth arm ( $p=3$ ). The phase distribution on each arm is optimized to radiate the beam according to the desired mask. Each mask has a circular contours defined in the direction of each beam with HPBW of  $5^\circ$  and  $-30 \text{ dB} \leq \text{SLL} \leq -20 \text{ dB}$ . The estimated radiation pattern shows that the SLL is below  $-17 \text{ dB}$ . The optimized phase distribution of the elements in each arm is used as a starting point for the PSO to radiate four beams in the same time. Figure 15 shows the mask and the estimated radiation pattern of the four beams simultaneous beam at  $\theta_{1,2,3,4}=30^\circ$ , and  $\phi_1=0^\circ$ ,  $\phi_2=90^\circ$ ,  $\phi_3=180^\circ$ , and  $\phi_4=270^\circ$ . The estimated quad-beam patterns have SLL below  $-25 \text{ dB}$ .

## 4.2 3-D Spherical Helical Array

Another 3D conformal helical array is the spherical arrangement with four quadrature arms shown in Fig. 16. A coordinates of each element is calculated from

$$\begin{aligned}
 x &= a \sqrt{1 - \Psi^2} \cos(\phi + \pi p/2) \\
 y &= a \sqrt{1 - \Psi^2} \sin(\phi + \pi p/2) \\
 z &= a \Psi
 \end{aligned} \tag{12}$$

where  $a$  is the radius of the sphere,  $\Psi = \frac{\theta}{\pi N}$ ,  $-\pi M \leq \theta \leq \pi M$ , and turns. The array has radius of  $5\lambda$  and six-turn helix with orthogonally oriented four arms. Figure 17 shows the estimated patterns of a single beam radiated from each arm of the spherical helical array designed in directions of  $\phi_1=0^\circ$ ,  $\phi_2=90^\circ$ ,  $\phi_3=180^\circ$ , and  $\phi_4=270^\circ$ . By optimizing the phases of the elements on each arm array radiates field with SLL of  $-16.4 \text{ dB}$ . Figure 18 shows the radiation pattern of the four beams simultaneously from the array at different directions.

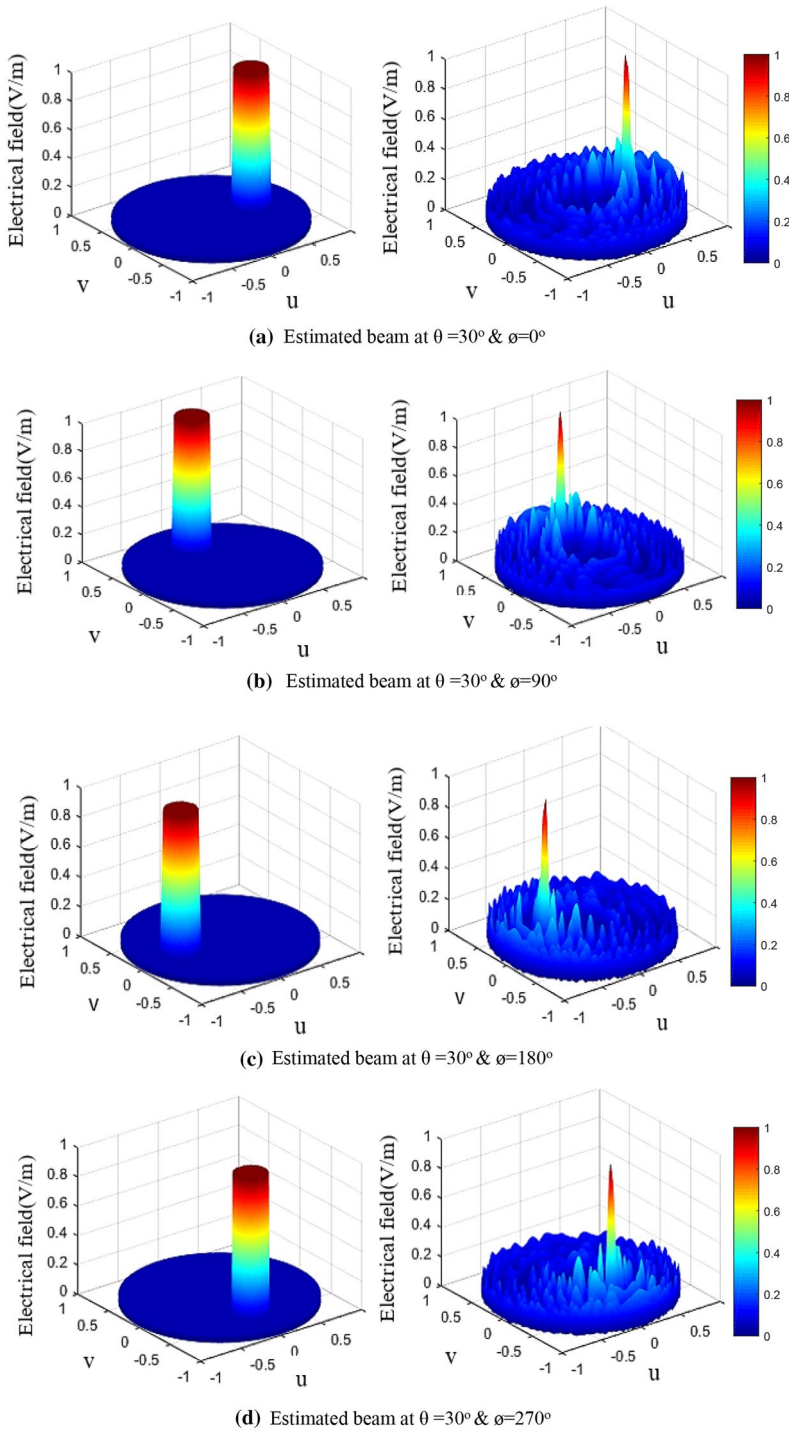


**Fig. 14** The 3D synthesized pencil beam patterns for each arm and the corresponding masks

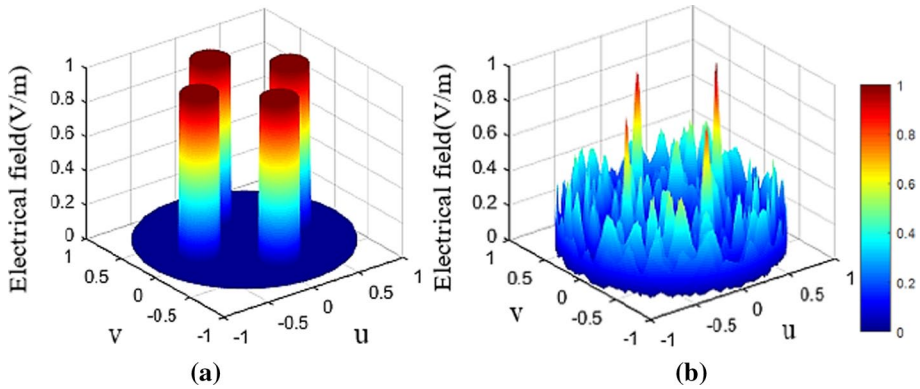


**Fig. 15** The 3D synthesized patterns with four pencil beam and the corresponding mask

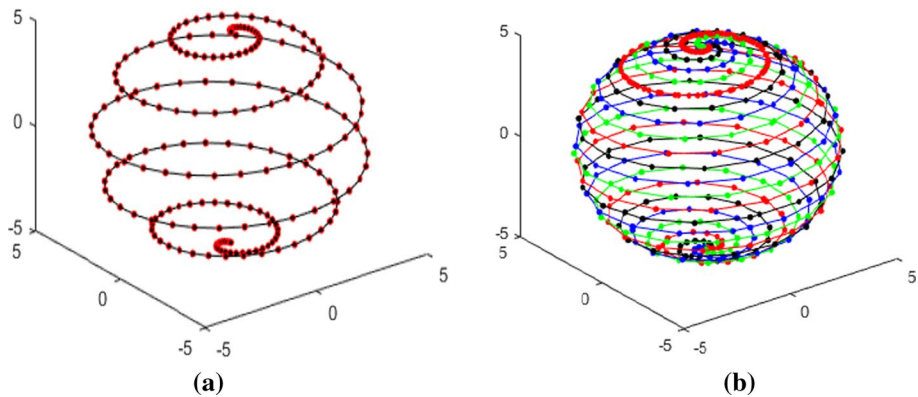


**Fig. 16** The 3D spherical helical antenna array **a** single arm, **b** four-orthogonal arms

## 5 Conclusion

This paper investigates the beam synthesis of 2D planar and 3D conformal array using PSO. By proper selection of the phase distribution on array elements and equal feeding the required beam is produced. A predetermined 2D and 3D masks are designed with specific HPBW and SLL. A 2D sunflower array arrangement is designed to produce single pencil beam with HPBW of  $20^\circ$  and flat-top beam with HPBW of  $60^\circ$  and cosecant square beam. Based on the PSO optimized phases dual similar pencil and flat-top beams are produced at  $\theta = -25^\circ$  and  $\theta = +25^\circ$ . The array is optimized for 3D masks with pencil and flat-top beams. 3D conformal helical array arranged in cylindrical and spherical geometry are investigated. Each array consists of four quadrature arms designed to produce four quadrature beams at  $\phi_1 = 0^\circ$ ,  $\phi_2 = 90^\circ$ ,  $\phi_3 = 180^\circ$ , and  $\phi_4 = 270^\circ$ . The SLL of  $-17$  dB is obtained for the four beam.

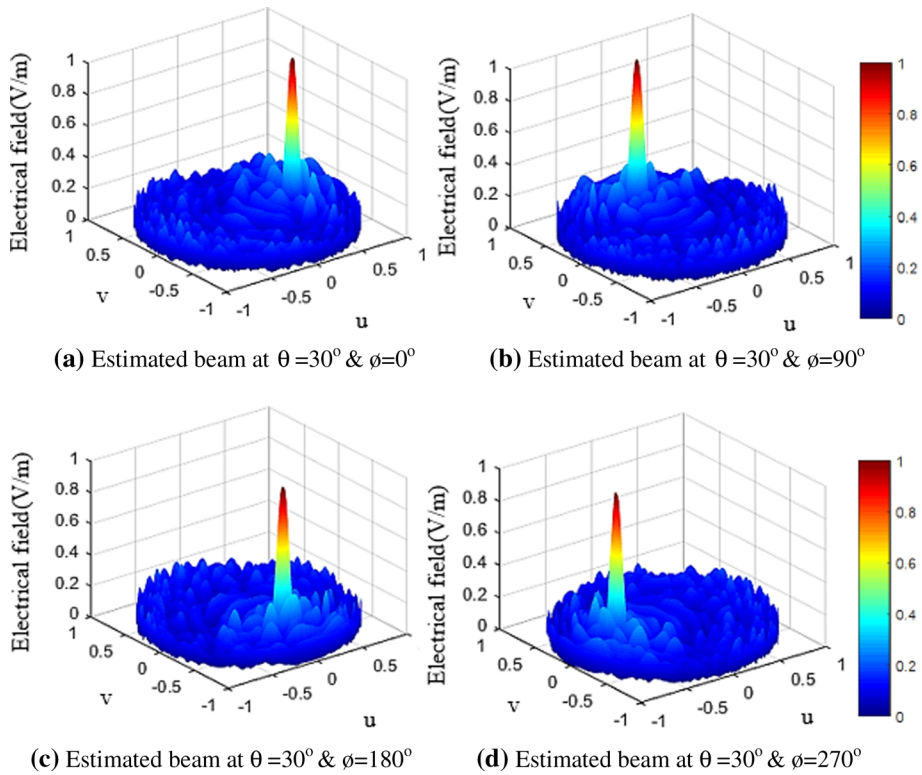


**Fig. 17** The 3D synthesized pencil beam patterns for each arm and the corresponding masks

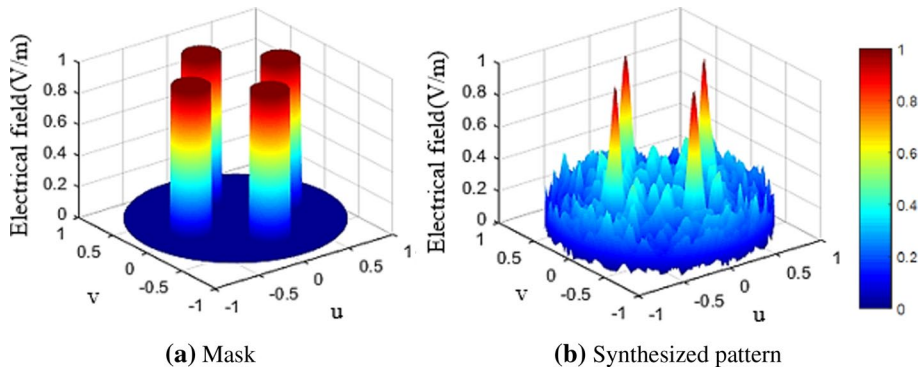


**Fig. 18** The 3D synthesized four pencil beams patterns and corresponding mask for the spherical helical array

## References

1. Bellofiore, S., Balanis, C. A., Foufz, J., & Spanias, A. S. (2002). Smart antenna systems for mobile communication networks. *IEEE Antennas and Propagation Magazine*, 44(3), 145–154.
2. Bucci, O. M., Mazzarella, G., & Panariello, G. (1991). Reconfigurable arrays by phased-only control. *IEEE Transactions on Antennas and Propagation*, 39(7), 919–925.
3. Marcano, D., & Durán, F. (2000). Synthesis of antenna arrays using genetic algorithms. *IEEE Antennas and Propagation Magazine*, 42(3), 12–20.
4. Morabito, A. F., Massa, A., & Isernia, T. (2012). An effective approach to the synthesis of phased-only reconfigurable linear arrays. *IEEE Transactions on Antennas and Propagation*, 60(8), 3622–3631.
5. Liu, Y., Nie, Z., & Liu, Q. H. (2010). A new method for the synthesis of non-uniform linear arrays with shaped power patterns. *Progress In Electromagnetics Research*, 107, 349–363.
6. Žilinskis, A., & Zhigljavsky, A. (2016). Stochastic global optimization: A review on the occasion of 25 years of Informatica. *Informatica*, 27(2), 229–256.
7. Mailloux, R. J. (1994). *Phased array antenna handbook*. Norwood: Artech House.
8. Bataineh, M. H., & Ababneh, J. I. (2006). Synthesis of aperiodic linear phased antenna arrays using particle swarm optimization. *Electromagnetics*, 26, 531–541.
9. Viganó, M. C., et al. (2009). Sunflower array antenna with adjustable density taper. *International Journal of Antennas and Propagation*, 2009, 1–10.
10. Fakher, M. A. (2015). Pattern synthesis for a conformal array antenna mounted on a paraboloid reflector using genetic algorithms. *Applied Computational Electromagnetics Society Journal*, 30(2), 230–236.
11. Speciale, R. A. (1994). Conformal phased array antenna. U.S. Patent No. 5,347,287.
12. Josefsson, L., & Patrik, P. (2006). *Conformal array antenna theory and design* (Vol. 29). New York: Wiley.
13. Azzam, D. M., Malhat, H. A., & Zainud-Deen, S. H. (2018, March). Phased-only pattern synthesis for sunflower and conformal arrays with shaped radiation patterns. In *2018 35th National Radio Science Conference (NRSC)* (pp. 30–37). IEEE.
14. Kennedy, J., & Eberhart, R. (1995). Particle swarm optimization. In *IEEE international conference on neural networks, Perth* (pp. 1942–1948). Piscataway, NJ: IEEE Service Center.
15. Mahmoud, K. R. (2008). Analysis of smart antenna arrays using optimization techniques. Ph.D. Thesis, Faculty of Engineering, Helwan University, Egypt.
16. Malhat, H., & Zainud-Deen, S. (2017). Linearly and circularly polarized reflectarray antennas with 4-arm archimedean spiral lattice. In *32nd URSI general assembly and scientific symposium (GASS)*, Montreal.
17. Niaz, M. W., Ahmed, Z., & Ihsan, M. B. (2016). Reflectarray with logarithmic spiral lattice of elementary antennas on its aperture. *International Journal of Electronics and Communications (AEU)*, 70(8), 1050–1054.
18. Dey, K. K., & Singh, D. P. (1986). Three dimensional helical shaped antenna array of half-wave dipole radiators. In *Proc. Indian national science academy* (Vol. 53, No. 3, pp. 373–384).
19. Alsawaha, H. W., & Safaai-Jazi, A. (2010). Ultra-wideband hemispherical antennas. *IEEE Transactions on Antennas and Propagation*, 58(10), 3175–3181.

**Publisher's Note** Springer Nature remains neutral with regard to jurisdictional claims in published maps and institutional affiliations.



**Saber Helmy Zainud-Deen** was born in Menouf, Egypt, on November 15, 1955. He received the B.Sc. and M.Sc. degrees from Menoufia University in 1973 and 1982 respectively, and the Ph.D. degree in antenna engineering from Menoufia University, Egypt in 1988. He is currently a professor in the department of electrical and electronic engineering in the faculty of electronic engineering, Menoufia University, Egypt. His research interest at present include microstrip and leaky wave antennas, DRA, RFID, optimization techniques, FDFD and FDTD, scattering problems and breast cancer detection.



**Doaa Mohammed Zaki Azzam** was born in Menouf, Egypt, on August 12, 1990. She received the B.Sc. degree from Menoufia University in 2012. She is currently working for M.Sc. degree in Antenna Engineering from Menoufia University, Egypt. Her research interest at present antenna arrays, beam shaping, and smart antenna.



**Hend Abd El-Azem Malhat** was born in Menouf, Egypt, on December 12, 1982. She received the B.Sc. and M.Sc. degrees from Menoufia University in 2004 and 2007 respectively. She received her Ph.D. degree in Antenna Engineering from Menoufia University, Egypt 2011. She is currently an associated professor in the department of electrical and electronic engineering in the faculty of electronic engineering, Menoufia University, Egypt. Her research interest at present include Graphene antennas, plasma antennas, wavelets technique, transmitarray, reflectarray and RFID.